Electronic Supplementary Material (ESI) for Energy & Environmental Science.

Supporting information

A Low Temperature Molten Salt Process for Aluminothermic Reduction of Silicon Oxides to Crystalline Si for Li-ion batteries

Ning Lin, Ying Han, Jie Zhou, Kailong Zhang, Tianjun Xu, Yongchun Zhu,* and Yitai Qian*

Department of Chemistry and Hefei National Laboratory for Physical Science at Micro-scale, University of Science and Technology of China, Hefei, Anhui 230026, (P. R. China)

Experimental section

Materials synthesis

All reagents were used without further purification. All the chemical reagents were purchased from Sinopharm Chemical Reagent Co. Ltd. In a typical procedure, $AlCl_3$ (8.00 g), aluminium (Al) powder (0.8 g), and high 1.0 g of high silica zeolite (SMF-400S, Shanghai FUYU New Material Technology Co., Ltd) were mixed and loaded in a stainless steel autoclave (volume 20 mL). The above procedure was conducted in a glove-box filled with N_2. Then, the autoclave was sealed immediately and heated in an electric stove with a heating ramp rate of 5 $^oC\ min^{-1}$ and maintained at 200 ^oC or 250 ^oC for 10 h. After cooling to room temperature naturally, the products were collected and washed with 0.1 M hydrochloric acid (HCl), distilled water, and ethanol for several times. The obtained sample was then immersed in diluted ethanol-based hydrofluoric acid (HF) solution for 3.0 min to remove the residual silicon oxides. Finally, the product was dried in vacuum oven at 50 ^oC for 1 h for further characterization. The reduction of commercial SiO_2, kieselguhr, albite, and fiberglass are carried out at 250 ^oC with the same weight ratio of the reagents including metallic Al and $AlCCl_3$. The reduction of high silica zeolite with excess metallic magnesium (Mg) was also carried out at 200 ^oC. To clear observe the reaction status, the experiment

concerning the reduction of zeolite with Al in presence of $AlCl_3$ was also conducted in sealed quartz tubes reactor.

Characterization

The structure and morphology of the product were characterized by X-ray diffractometer (Philips X' Pert Super diffract meter with Cu Kα radiation (λ=1.54178 Å)), Raman spectrometer (Lab-RAM HR UV/VIS/NIR), X-ray photoelectron spectroscopy (XPS) (ESCA-Lab MKII X-ray photoelectron spectrometer), scanning electron microscopy (SEM, JEOL-JSM-6700F), and transmission electron microscopy (TEM, Hitachi H7650 and HRTEM, JEOL 2010).

Electrochemical Measurement

The electrochemical properties of the prepared Si sample were evaluated through coin-type cells (2016 R-type) which were assembled under an argon-filled glove box (H_2O, O_2 < 1 ppm). Metallic Li sheet was used as counter and reference electrode. 1 M $LiPF_6$ in a mixture of ethylene carbonate/dimethyl carbonate (EC/DMC; 1:1 by volume) was served as the electrolyte (Zhuhai Smooth way Electronic Materials Co., Ltd (china)). For preparing working electrode, the slurry mixed with as-prepared active Si material, carbon black (super P) and sodium alginate (SA) binder in a weight ratio of 6:2:2 in water solvent was pasted onto a Cu foil, and then dried in a vacuum oven at 80 ^oC for 10 h. The active material density of each electrode was determined to be about 1.0 mg cm^{-2}. Galvanostatic measurements were conducted using a LAND-CT2001A instrument at room temperature with a fixed voltage range of 0.005−1.5 V (*vs.* Li/Li^+). Cyclic voltammetry (CV) was performed on electrochemistry workstation (CHI660D), with a scanning rate of 0.2 mV s^{-1} at room temperature.

(1)

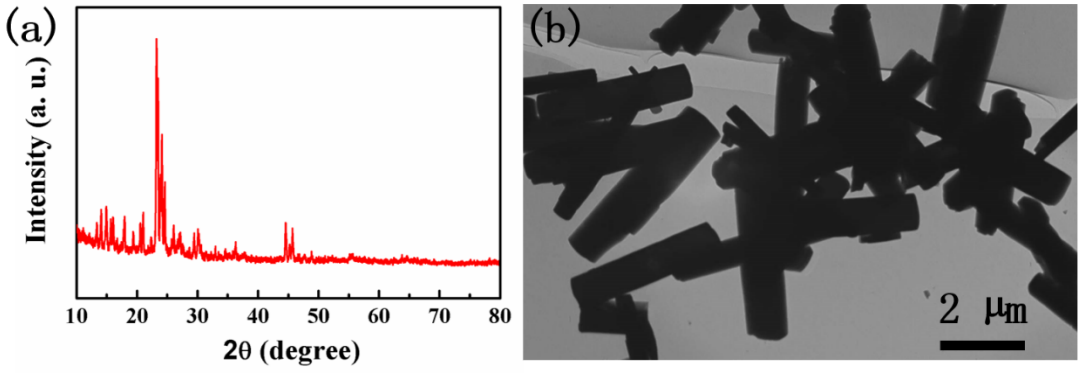

Figure S1. The (a) XRD patterns and the (b) SEM image of the commercial high silica zeolite, the main content is aluminium silicate ($Al_2O_3/11SiO_2$) (JCPDS No. 44-0003).

(2) The effect of reaction temperature on the reduction with Al in molten AlCl3 was studied, as shown in Figure S2. It is obvious that the reaction could be initiated to generate Si nanoparticles at 200 °C. At 250 °C, the peaks of the crystalline zeolite are disappeared completely, implying more sufficient reduction. Meanwhile, the yield increases from 40% at 200 °C to 75% at 250 °C, while no significant change of yield is detected at 300 °C.

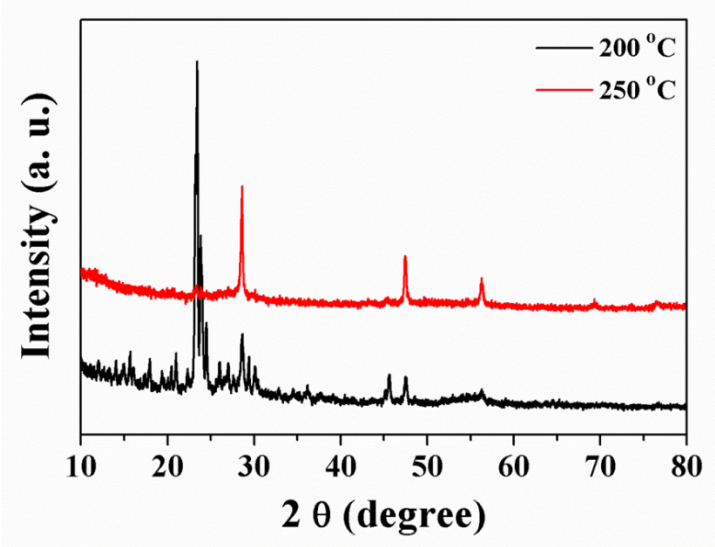

Figure S2. The (a) XRD patterns of the product prepared at 200 °C, and 250 °C. The temperature effect on the reduction process is studied by conducting the experiment at 200 °C, and 250 °C, respectively. The obtained products were washed with 0.1 M hydrochloric acid (HCl), distilled water, and ethanol, but without the HF solution. The above picture shows the corresponding XRD patterns.

(3)

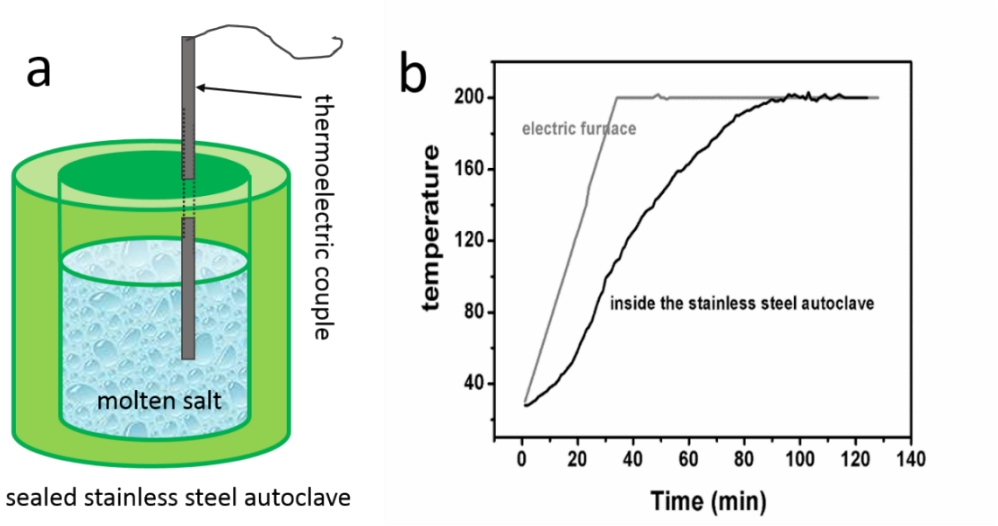

Figure S3. (a) The schematic picture of our self-made stainless steel autoclave for measuring the inner temperature variation. (b) The temperature change plots as a function of time inside the electric furnace and inside the stainless steel autoclave. The thermocouple thermometer is plugged into the stainless steel autoclave. Note that the autoclave must be sealed tightly.

(4) We conducted the experiments in a quartz tube to observe the reaction directly. After cooling to room temperature gradually, some crystal-like matter is condensed at the top of the tube, which is verified as pure $AlCl_3$ by XRD analysis.

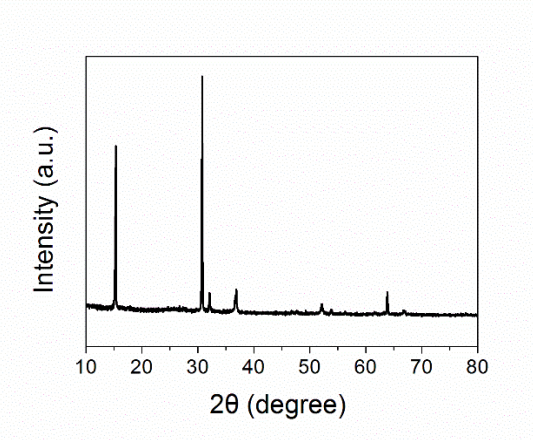

Figure S4. The XRD pattern of the sample obtained from the top side of the quartz tube. The main content is $AlCl_3$.

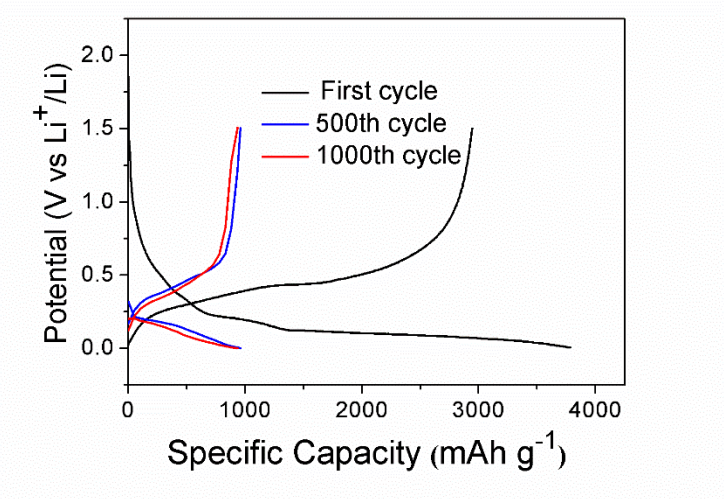

(5)

Figure S5. Discharge–charge voltage curves of 500th and 1000th cycles at a current density of 3 A g^{-1}. The first cycle is measured at 0.3 A g^{-1}. As we can see, the discharge/charge voltage-profiles are attributed to the typical Si anode. At high current density of 3A/g, the discharge plateaus of the Si based electrode at 500th and 1000th cycles are all located at below 0.2 V (vs. Li+/Li), During charge process, the voltage plateaus locate at between 0.3 and 0.5 V (vs. Li+/Li). Besides, the corresponding coulombic efficiency of both 500th and 1000th cycles are over 97% at 3 A g^{-1}.

(6)

The morphology variation of the as-prepared Si and the commercial micro-sized Si (Sinopharm Chemical Reagent Co. Ltd., 200 mesh) based electrodes are investigated before and after cycling. The below Figure S5 exhibits the SEM and enlarged SEM images, the un-cycled electrodes exhibit a uniform mixture of the active materials, binder, and carbon black. Both bulk Si and as-prepared nano-sized Si electrodes show relatively flat surface. Note that we can observe the active Si contents in the electrode clearly. Figure S6 shows

the cycled electrode. After 10 cycles, surface of all electrodes becomes smoother, which may result from the formation of solid state interface membrane. Figure S6 a, b display the SEM and enlarged SEM images of commercial bulk Si based electrode. Obviously, some protuberance and micro-sized hole on the electrode surface is formed, which may be caused by the huge volume change of the micro-sized bulk Si. As for as-prepared Si nanoparticles, electrode still presents flat surface (Figure S6c). We also disclosed the inner composition of the cycled electrode, as shown in Figure S6d**.** No independent Si nanoparticles could be observed, which may be caused by two aspects. First, the generated SEI membrane would cover on the particles. Second, it is well-accepted that the crystalline Si would converted into amorphous phase after repeated lithiation and de-lithiation process. After a few cycles, the origin structure may disappear, but still connect with binder and carbon black tightly. However, the bulk Si with drastic volume variation

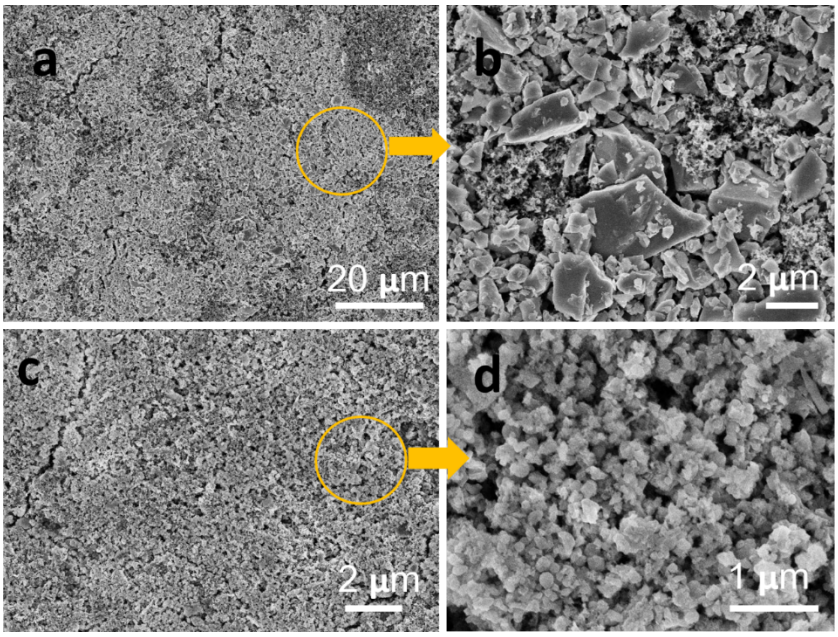

would loss contact with the current collector. So, it is reasonable to speculate that the nanostructured Si could effectively suppressing the volume change, leading to enhanced electrochemical performance.

Figure S6. The (a) SEM and enlarged SEM images of commercial bulk Si based electrode (before cycling). The (c) SEM and enlarged SEM images of as-prepared Si nanoparticles based electrode (before cycling).

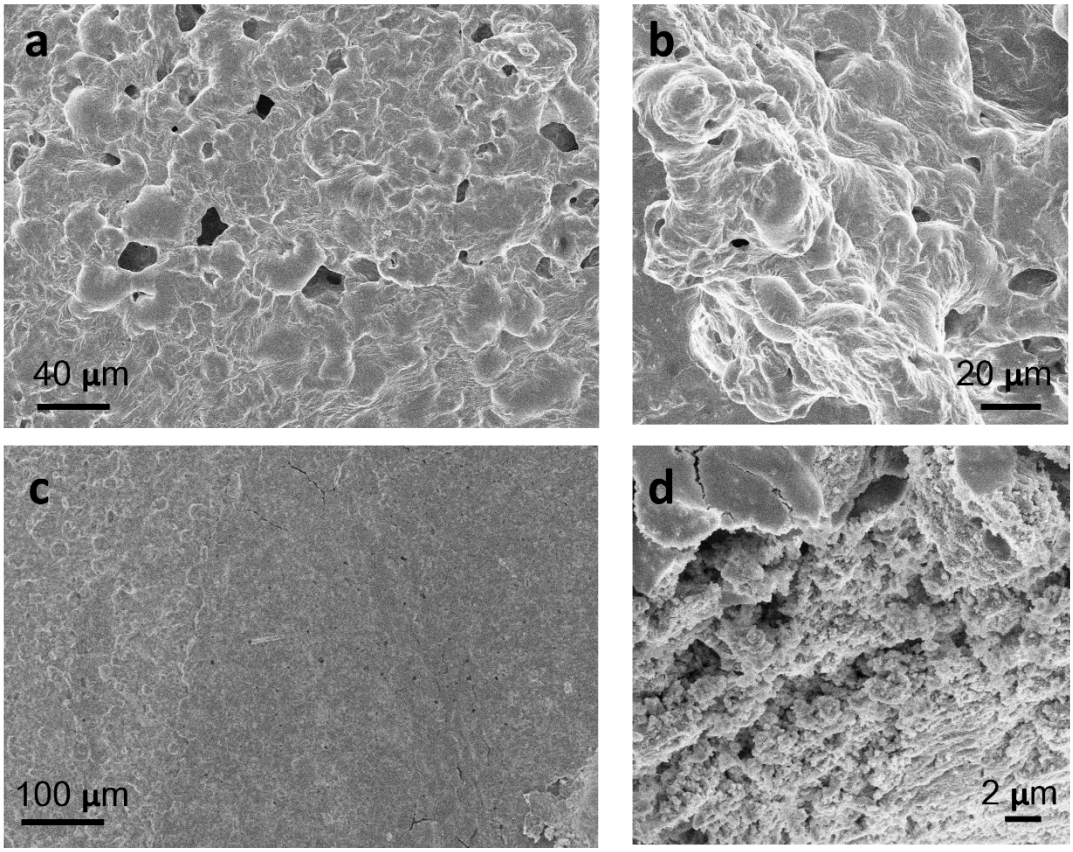

Figure S7. The (a) SEM and enlarged SEM images of commercial bulk Si based electrode (after 10 cycles). The (c) SEM and enlarged SEM images of as-prepared Si nanoparticles based electrode (after 10 cycles).

(7)

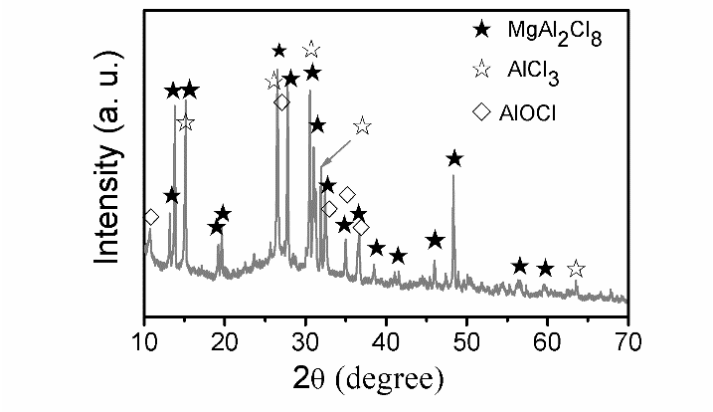

Figure S8. The XRD patterns of the crud products of the reaction between Mg, $AlCl_3$ and high silica zeolite. The existence of $AlCl_3$ (labeled as "☆", JCPDS No.77-0819) is attributed

to the excess reagent, providing liquid environment. A group of dominant diffraction peaks (labeled as "★") in the pattern can be characterized as complex chlorides $MgAl_2Cl_8$ (JCPDS No.78-0916) which is the main by-product. The peaks labeled as "◇"are assigned to the orthorhombic phase AlOCl (JCPDS No. 16-0448) that is the other important by-product. It is reasonable to speculate that both metallic Al and the molten salt AlCl3 participate the reduction process as: 2Mg + SiO2 + 6AlCl3 → 2MgAl2Cl8 + 2AlOCl + Si.

(8)

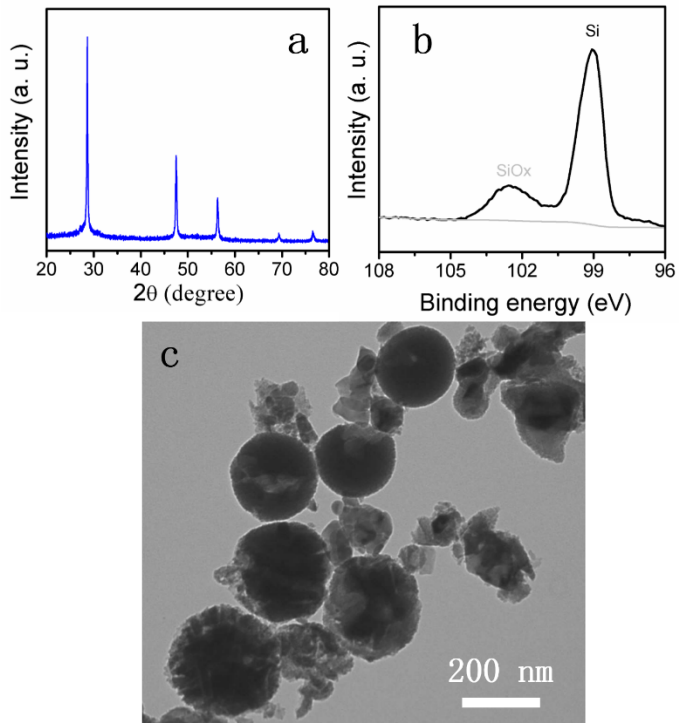

Figure S9. The (a) XRD patterns, (b) XPS, (c) TEM images of the Si prepared through reduction of commercial nano-sized SiO_2 precursor with Al in $AlCl_3$. The corresponding XRD patterns (Figure S9a) and XPS plot (Figure S9b) indicate that the obtained samples are well-crystallized Si (JCPDS 27-1402), with a small amount of amorphous SiO_x. The TEM image (Figure S9c) exhibits the Si sample consists of nano-sized particles.

(9)

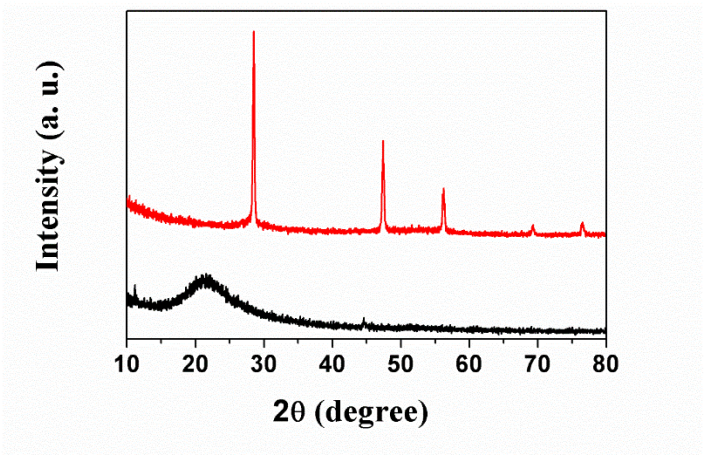

Figure S10. The XRD patterns of the Si prepared from fiberglass and the corresponding fiberglass precursor.

(10)

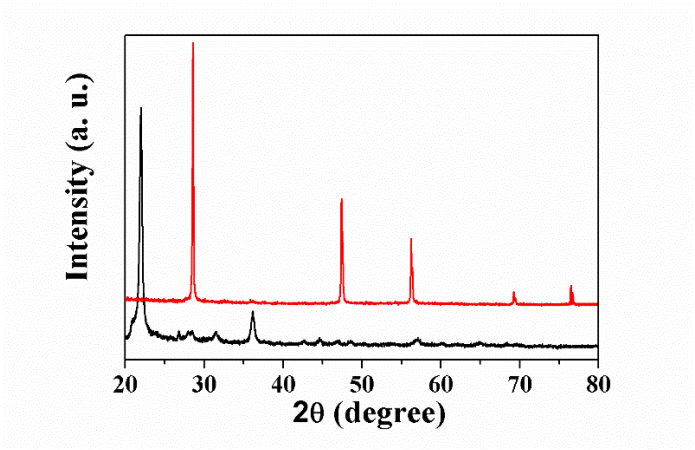

Figure S11. The XRD patterns of the Si prepared from kieselguhr and the corresponding kieselguhr precursor.

(11)

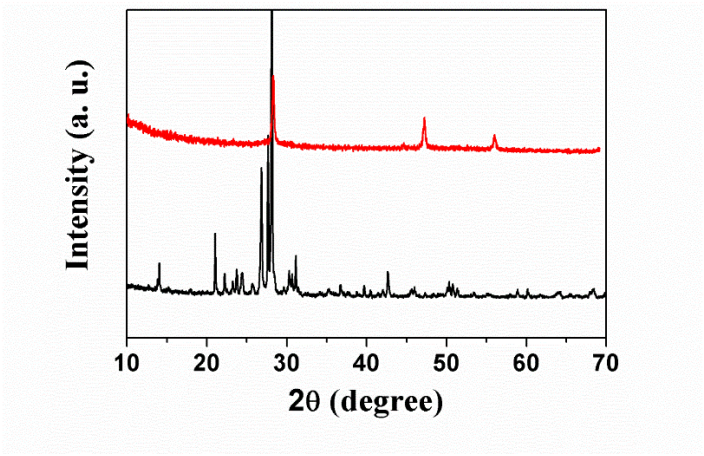

Figure S12. The XRD patterns of the Si prepared from mineral albite, and the corresponding albite precursor.